JMEPEG (2012) 21:47–54
DOI: 10.1007/s11665-011-9868-5

1059-9495/$19.00

Effects of Minor Zr and Sr on As-Cast Microstructure and Mechanical Properties of Mg-4Y-1.2Mn-1Zn (wt.%) Magnesium Alloy

Mingbo Yang, Fusheng Pan, Jia Shen, Tao Zhou, and Caiyuan Qin

(Submitted October 5, 2010; in revised form December 17, 2010)

The effects of minor Zr and Sr on the as-cast microstructure and mechanical properties of the Mg-4Y-1.2Mn-1Zn (wt.%) alloy were investigated using optical and electron microscopies, differential scanning calorimetry (DSC) analysis, and tensile and creep tests. The microstructural results indicate that small additions of Zr and/or Sr to the Mg-4Y-1.2Mn-1Zn alloy do not cause an obvious change in the morphology and distribution of the $Mg_{12}YZn$ phase in the alloy. The tensile and creep tests indicate that, although small additions of Zr and/or Sr to the Mg-4Y-1.2Mn-1Zn alloy do not have obvious effects on the creep properties of the alloy, the tensile properties at room temperature and 300 °C for the alloys added with Zr and/or Sr are improved. Among the Zr- and/or Sr-containing alloys, the alloy specifically added with of 0.5 wt.% Zr + 0.1 wt.% Sr obtains the optimum tensile properties, and is followed by the alloys added with 0.5 wt.% Zr and 0.1 wt.% Sr.

Keywords grain refinement, magnesium alloy, Mg-Y-Mn-Zn alloy, Zr and Sr additions

1. Introduction

At present, the development of new magnesium alloys is becoming increasingly important owing to the potential saving in weight when compared with aluminum-based alloys. However, the creep properties of magnesium alloys are limited by their low melting point which can vary depending on the alloying content (Ref 1). Hence, the development of magnesium alloys of elevated temperature is necessary to compete with other light constructional materials such as aluminum alloys, and to improve the temperature range of application of magnesium components. Previous investigations indicated that magnesium alloys based on the Mg-Sc system exhibited interesting properties (Ref 2, 3), and it was further found that the additions of Mn and Y to Mg-Sc alloys could improve the creep resistance substantially (Ref 4, 5). For example, the quaternary Mg-Y-Mn-Sc alloys are considerably superior to WE alloys and exhibit high creep resistance at high temperatures over 300 °C (Ref 5, 6). However, owing to the expensive scandium, the application of the Mg-Y-Mn-Sc alloys is limited. Therefore, the research of replacing expensive scandium by cheaper alloying elements for the Mg-Y-Mn-Sc alloys needs to be considered. Previous investigations about Mg-Y-Zn high strength alloys found that Zn can form intermetallic phases with Mg and/or RE as plates on basal planes of α-Mg matrix (Ref 7-9). In addition, Smola et al. (Ref 10) found that the Mg-4Y-1Mn-1Zn alloy exhibited higher creep properties than the Mg-4Y-1Mn-1Sc alloy. Therefore, it was originally suggested that Zn is possibly the less expensive alternative to Sc in the Mg-Y-Mn-Sc alloys. However, further investigations found that, similar to the quaternary Mg-Y-Mn-Sc alloys, the microstructures of the quaternary Mg-Y-Mn-Zn alloys also are relatively coarse, thus leading to the relatively poor mechanical properties (Ref 10, 11). Therefore, further enhancement in the mechanical properties for the quaternary Mg-Y-Mn-Zn alloys by microstructural refinement needs to be considered.

It is well known that Zr is a powerful grain refiner for Mg-RE magnesium alloys to further improve the mechanical properties, and the Zr-containing magnesium alloys usually show a higher corrosion resistance than the Zr-free magnesium alloys (Ref 12). In addition, it is also known that the Sr addition can refine the microstructures, and improve the strength and creep resistance of magnesium alloys (Ref 13, 14), and Zhao et al. (Ref 15) found that adding minor amount of Sr to the Mg-3.5Mn alloy could refine the grains of the alloy and thus lead to the improvement of the tensile strength and toughness. Although it has been reported that Zr could not be used in the Mn-containing magnesium alloys (Ref 16, 17), it has not been supported with powerful evidence, and some Mn- and Zr-containing magnesium alloys such as Mg-Y-Mn-Zr alloys are being developed (Ref 18, 19). Therefore, it is expected that the Zr and/or Sr additions to the Mg-Y-Mn-Zn alloy are possibly beneficial to the microstructural refinement and the improvement of mechanical properties. Owing to the above mentioned reasons, this study investigates the effects of minor additions of Zr and/or Sr on the as-cast microstructures and mechanical properties of the Mg-4Y-1.2Mn-1Zn magnesium alloys.

Mingbo Yang, Jia Shen, Tao Zhou, and **Caiyuan Qin**, Materials Science & Engineering College, Chongqing University of Technology, Chongqing 400050, China; **Mingbo Yang** and **Fusheng Pan**, National Engineering Research Center for Magnesium Alloys, Chongqing University, Chongqing 400030, China; and **Mingbo Yang**, Key Laboratory of Automobile Components Manufacturing and Testing Technology of the Education Ministry, Chongqing University of Technology, Chongqing 400054, China. Contact e-mail: yangmingbo@cqut.edu.cn.

2. Experimental Procedures

The experimental alloys with different compositions (Table 1) were prepared from commercially pure Mg and Zn (>99.9 wt.%), and Mg-17 wt.%Y, Mg-4.38 wt.%Mn, Mg-31.27 wt.%Zr, and Mg-10 wt.%Sr master alloys supplied by Hunan Rare Earth Metal & Material Institute, China. The experimental alloys were made to melt in a crucible resistance furnace, protected by 2 wt.% RJ-2 flux additions (45 wt.% $MgCl_2$ + 37 wt.% KCl + 8 wt.% NaCl + 4 wt.% CaF_2 + 6 wt.% BaCl). After being held at 740 °C for 20 min, the melts of the experimental alloys were separately homogenized by mechanical stirring at 300 rpm for 2 min, and then poured into a permanent mould which was coated with 6 wt.% pulvistalci water-based paint and preheated to 200 °C to obtain a casting as shown in Fig. 1. Similar to the previous investigations (Ref 20), in order to save materials and costs, the specimens as shown in Fig. 2 were fabricated from the castings for tensile and creep tests. Furthermore, the samples of the experimental alloys were subjected to a solution heat treatment (520 °C/12 h + water cooled) to reveal the grain boundaries and examine the microstructural stability at high temperatures. Table 1 lists the actual chemical compositions of the experimental alloys, which were inspected by inductively coupled plasma spectroscopy.

In order to analyze the solidification behavior of the experimental alloys, the differential scanning calorimetry (DSC) was carried out by using a NETZSCH STA 449C system equipped with platinum-rhodium crucibles. Samples weighted around 30 mg were first heated to 700 °C in a flowing argon atmosphere, and then held at 700 °C for 5 min before being cooled down to 100 °C. The heating and cooling curves were recorded at a rate of 15 °C/min.

The as-cast and solutionized samples of the experimental alloys were respectively etched in an 8% nitric acid solution in distilled water and a solution of 1.5 g picric, 25 mL ethanol, 5 mL acetic acid, and 10 mL distilled water, and then were examined using an Olympus optical microscope and/or JEOL JSM-6460LV type scanning electron microscope equipped with Oxford energy dispersive x-ray spectrometer (EDS) with an operating voltage of 20 kV. The phases in the experimental alloys were analyzed using D/Max-1200X type x-ray diffraction (XRD) operated at 40 kV and 30 mA with Cu Kα radiation, a step scanning 2θ from 20° to 80°, a step size of 0.03°, and a count time of 3 s. The phases in the experimental alloys were determined using a PDF2 database. The grain size was analyzed by the standard linear intercept method using an Olympus stereomicroscope. The as-cast tensile properties of the experimental alloys at room temperature and 300 °C were determined from a complete stress-strain curve. Ultimate tensile strength (UTS), 0.2% yield strength (YS), and elongation to failure (Elong.) were obtained based on the average value of three tests. Constant-load tensile creep tests were performed at 300 °C and 30 MPa for creep extension up to 100 h. The minimum creep rates of the as-cast experimental alloys were measured from each elongation-time curve and averaged over three tests.

Table 1 Actual compositions of the experimental alloys, wt.%

Experimental alloys	Y	Mn	Zn	Zr	Sr	Mg
Mg-4Y-1.2Mn-1Zn	3.69	1.11	0.92	…	…	Bal.
Mg-4Y-1.2Mn-1Zn-0.5Zr	3.70	1.06	0.92	0.37	…	Bal.
Mg-4Y-1.2Mn-1Zn-0.1Sr	3.71	1.04	0.90	…	0.07	Bal.
Mg-4Y-1.2Mn-1Zn-0.5Zr-0.1Sr	3.67	1.10	0.91	0.41	0.08	Bal.

Fig. 1 Casting with the fabricated area of the samples for the mechanical properties tests

3. Results and Discussion

3.1 Effects on As-Cast Microstructure

Figure 3 shows the XRD results of the as-cast alloys. As shown in Fig. 3, all the alloys mainly consist of α-Mg phase and $Mg_{12}YZn$ phase (a long-period 18R-modulated structure; Ref 7), and the Mn_2Zr phase, which has been reported in the Mg-4Y-1Mn-1Zr alloy (Ref 17), is not observed in the XRD results of the Zr-containing alloys. This is possibly related to the low content of Zr in the experimental alloys. Actually, the formation of the phases in the as-cast alloys may be preliminarily explained by the DSC results. Figure 4 shows the DSC cooling curves of the as-cast alloys. It is found from Fig. 4 that the DSC cooling curves of the alloys are similar, with two main peaks of A and B in the cooling curves, indicating that small additions of Zr and/or Sr to the Mg-4Y-1.2Mn-1Zn alloy does not influence the types of the phase transformations of the alloy. Since the experimental alloys have the Y/Zn atomic

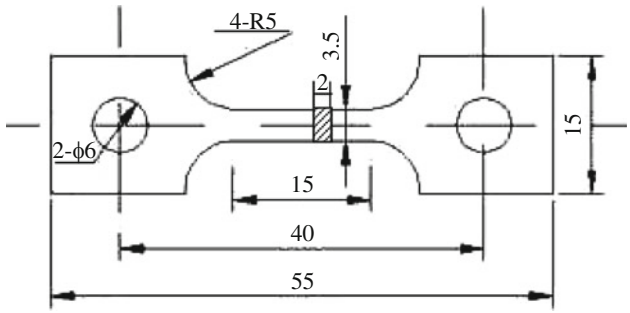

Fig. 2 Configuration of the samples used for the tensile and creep tests (unit: mm)

ratio of 2.94, its solidification process should be similar to the Mg-(2-3)Y-1Zn (at.%) alloys reported by Chen et al. (Ref 7) and Huang et al. (Ref 21). Based on the DSC results and the combined investigations of Chen et al. (Ref 7) and Huang et al. (Ref 21), it is preliminarily inferred, during the solidification of the experimental alloys, that the primary α-Mg phase first nucleates and grows at about 640 °C corresponding to the peak A. Then, along with the temperature decrease, a binary eutectic reaction ($L_1 \rightarrow$ α-Mg + $Mg_{12}YZn$) occurs at about 530 °C corresponding to the peak B. Accordingly, the final microstructures are mainly composed of α-Mg and $Mg_{12}YZn$ phases.

Figure 5 shows the optical images of the as-cast alloys. It is observed that the primary α-Mg phases in all the alloys mainly display a dendrite configuration. At the same time, it is found from Fig. 5 that the dendrite arm spacings of the primary α-Mg phases in the Zr and/or Sr-containing alloys are relatively smaller than those in the quaternary alloy. Furthermore, there is a trend toward a more equiaxed structure for the Zr and/or Sr-containing alloys especially for the Zr-containing alloys, which is further confirmed from Fig. 6. The above results indicate that small additions of Zr and/or Sr to the Mg-4Y-1.2Mn-1Zn alloy possibly refine the microstructure of the alloy. However, this needs to be further confirmed. In addition, it is observed from Fig. 6 that the grains of the Zr- and/or Sr-containing solutionized alloys are relatively finer than the quaternary solutionized alloy. The average grain size is 186 μm (the standard error: 15 μm) for the quaternary solutionized alloy, and after adding Zr and/or Sr, its average size is 102 μm (the standard error: 10 μm), 139 μm (the standard error: 12 μm), and 83 μm (the standard error: 13 μm) for the solutionized alloys with the additions of 0.5 wt.% Zr, 0.1 wt.% Sr, and 0.5 wt.% Zr + 0.1 wt.% Sr, respectively. It is known that the grain growth possibly happens after a solution heat treatment. Therefore, although the difference in the average grain size of the solutionized alloys is very obvious, it is not completely confirmed that small additions of Zr and/or Sr can refine the grains of the as-cast Mg-4Y-1.2Mn-1Zn alloy. The issue will be a subject for further study by our group.

Figure 7 shows the SEM images of the as-cast alloys. In Fig. 7, the second phases are identified according to the XRD and EDS analysis. As shown in Fig. 7, the $Mg_{12}YZn$ phases in all the alloys mainly exhibit continuous and/or quasi-continuous nets, and distribute at the grain boundary. Obviously, the morphology and distribution of the $Mg_{12}YZn$ phase in the Mg-4Y-1.2Mn-1Zn alloy are not significantly influenced by small additions of Zr and/or Sr. In addition, as shown in Fig. 7(b) and (f), the fine particle-like $Mg_{24}Y_5$ phase is also observed although the phase is not identified in the XRD results (Fig. 3). This is possibly related to the small amount of the phase.

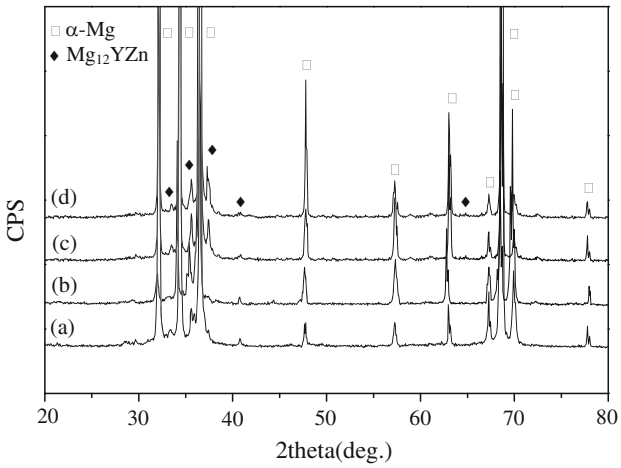

Fig. 3 XRD results of the as-cast alloys: (a) Mg-4Y-1.2Mn-1Zn; (b) Mg-4Y-1.2Mn-1Zn-0.5Zr; (c) Mg-4Y-1.2Mn-1Zn-0.1Sr; and (d) Mg-4Y-1.2Mn-1Zn-0.5Zr-0.1Sr

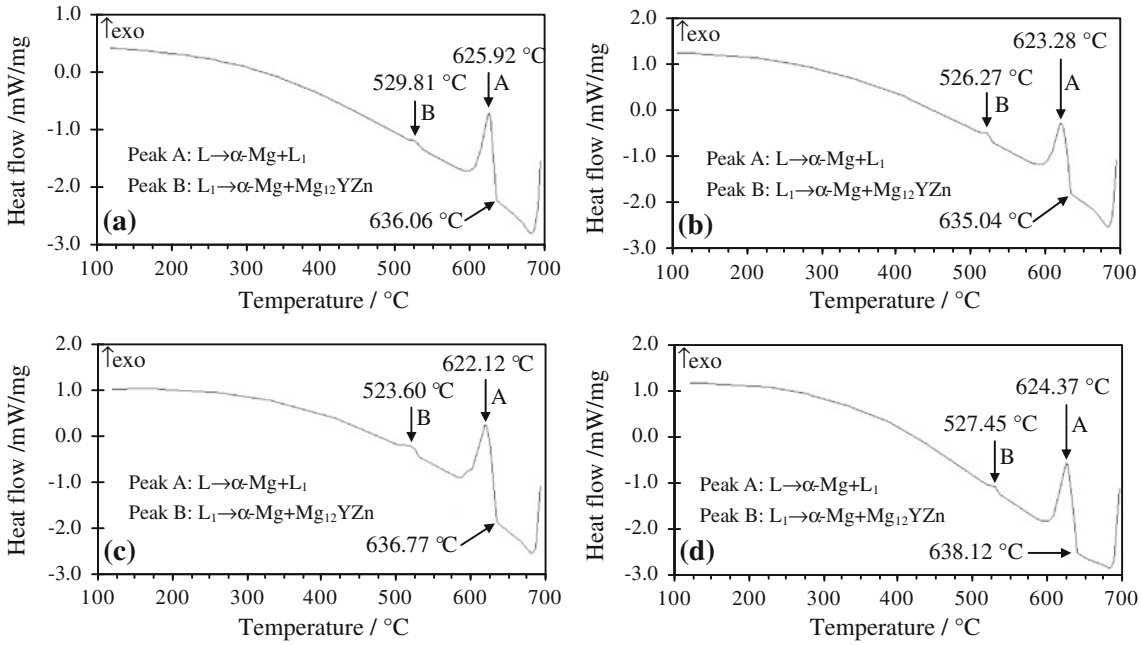

Fig. 4 DSC cooling curves of the as-cast alloys: (a) Mg-4Y-1.2Mn-1Zn; (b) Mg-4Y-1.2Mn-1Zn-0.5Zr; (c) Mg-4Y-1.2Mn-1Zn-0.1Sr; and (d) Mg-4Y-1.2Mn-1Zn-0.5Zr-0.1Sr

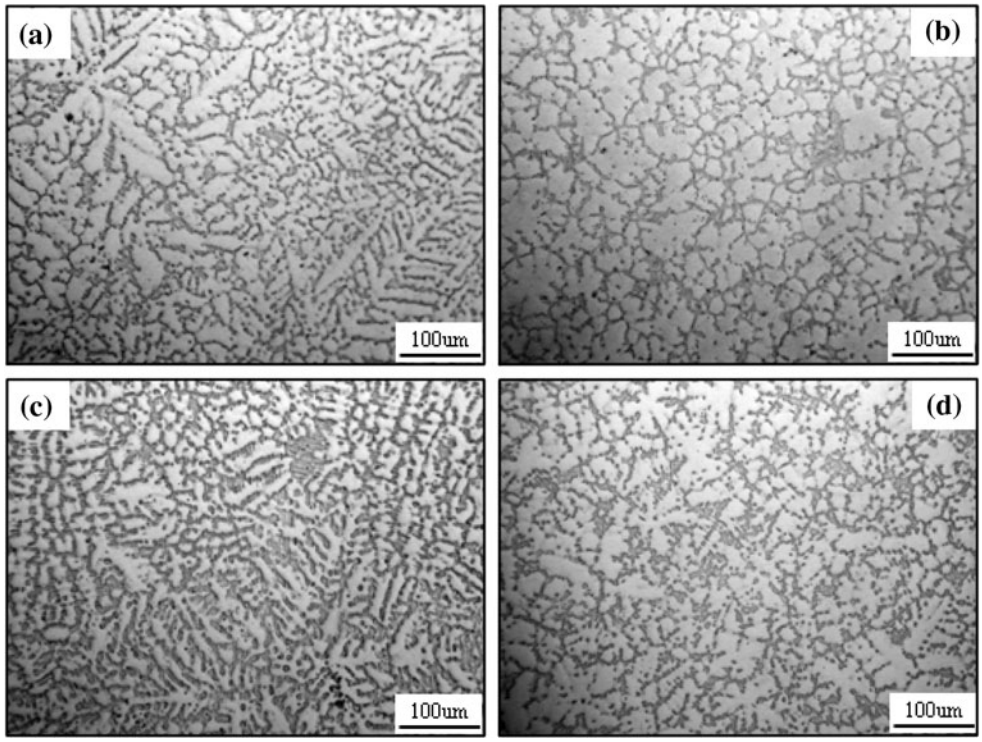

Fig. 5 Optical images of the as-cast alloys: (a) Mg-4Y-1.2Mn-1Zn; (b) Mg-4Y-1.2Mn-1Zn-0.5Zr; (c) Mg-4Y-1.2Mn-1Zn-0.1Sr; and (d) Mg-4Y-1.2Mn-1Zn-0.5Zr-0.1Sr

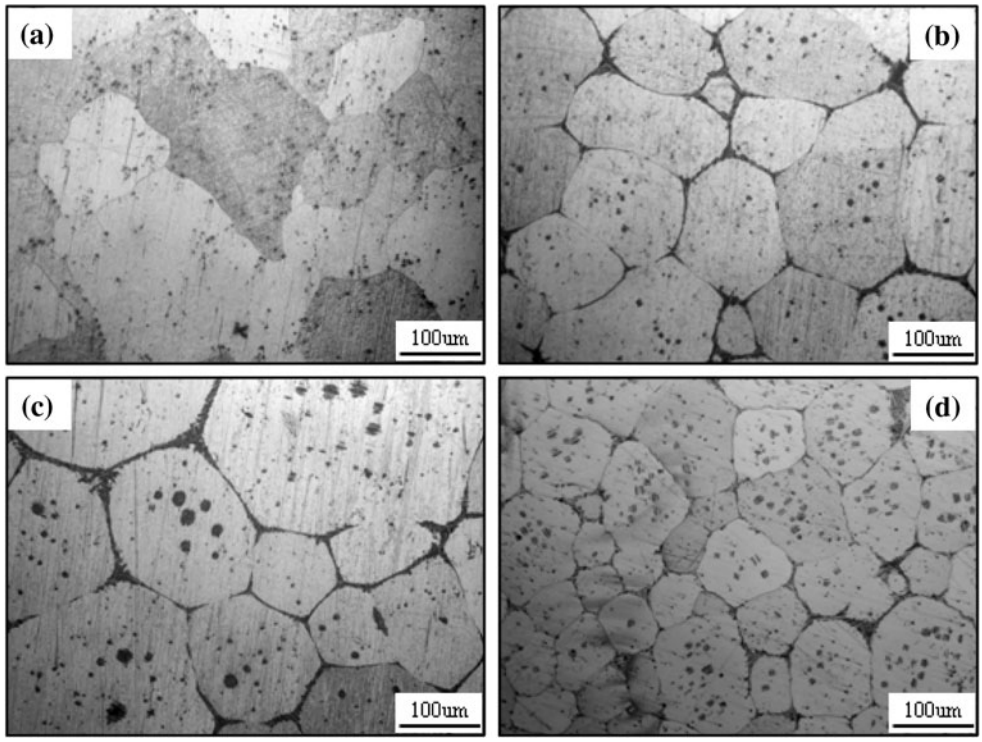

Fig. 6 Optical images of the solutionized alloys: (a) Mg-4Y-1.2Mn-1Zn; (b) Mg-4Y-1.2Mn-1Zn-0.5Zr; (c) Mg-4Y-1.2Mn-1Zn-0.1Sr; and (d) Mg-4Y-1.2Mn-1Zn-0.5Zr-0.1Sr

3.2 Effects on Mechanical Properties

The tensile properties, including ultimate tensile strength (UTS), 0.2% yield strength (YS), elongation (Elong.), and creep properties of the as-cast alloys are listed in Table 2. It is observed that the Zr- and/or Sr-containing alloys exhibit relatively higher tensile properties at the room temperature

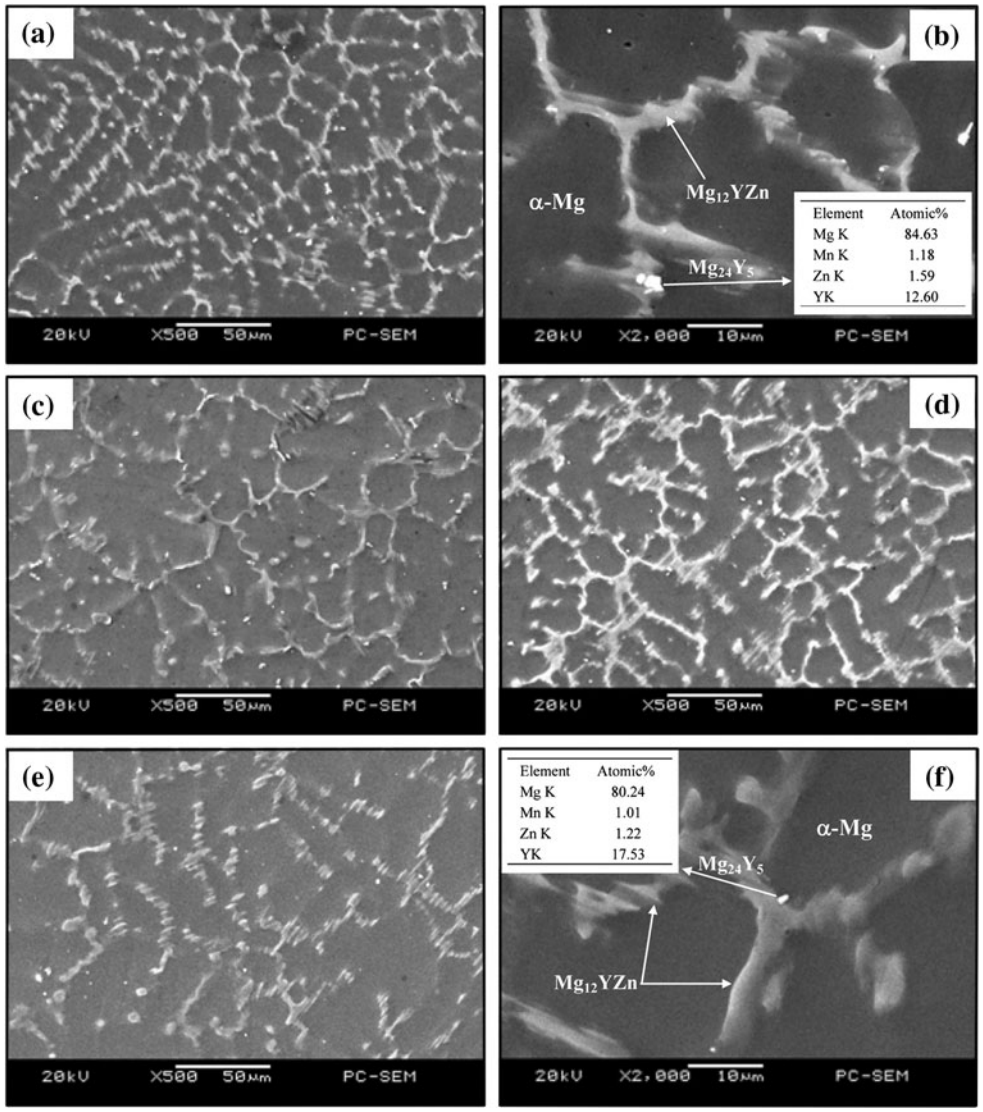

Fig. 7 SEM images of the as-cast alloys: (a, b) Mg-4Y-1.2Mn-1Zn; (c) Mg-4Y-1.2Mn-1Zn-0.5Zr; (d) Mg-4Y-1.2Mn-1Zn-0.1Sr; and (e, f) Mg-4Y-1.2Mn-1Zn-0.5Zr-0.1Sr

Table 2 Tensile and creep properties of the as-cast alloys

	Tensile properties						Creep properties	
	Room temperature			300 °C			300 °C and 30 MPa for 100 h	
Experimental alloys	UTS, MPa	YS, MPa	Elong., %	UTS, MPa	YS, MPa	Elong., %	Total creep strain, %	Minimum creep rate, $\times 10^{-9}$ s^{-1}
Mg-4Y-1.2Mn-1Zn	182 (3.7)	166 (2.9)	2.8 (0.31)	115 (3.2)	108 (3.3)	14.2 (0.78)	0.312 (0.08)	8.67 (0.18)
Mg-4Y-1.2Mn-1Zn-0.5Zr	199 (1.8)	179 (2.4)	3.3 (0.18)	134 (1.4)	116 (2.2)	16.8 (0.56)	0.300 (0.02)	8.34 (0.12)
Mg-4Y-1.2Mn-1Zn-0.1Sr	189 (3.2)	172 (1.1)	3.0 (0.25)	122 (2.3)	110 (2.6)	15.6 (0.61)	0.302 (0.04)	8.38 (0.17)
Mg-4Y-1.2Mn-1Zn-0.5Zr-0.1Sr	223 (2.9)	193 (1.9)	3.7 (0.22)	145 (1.2)	128 (3.4)	17.9 (0.65)	0.299 (0.03)	8.32 (0.21)

Note: the data in the bracket is the standard error

and 300 °C than the quaternary alloy, indicating that small additions of Zr and/or Sr to the Mg-4Y-1.2Mn-1Zn alloy is beneficial to the improvement of the tensile properties. Furthermore, it is found from Table 2 that among the Zr- and/or Sr-containing alloys, the tensile properties of the alloy with the addition of 0.5 wt.% Zr + 0.1 wt.% Sr are the highest, followed by the alloys with the additions of 0.5 wt.% Zr and 0.1 wt.% Sr, in the respective order. The effects of small

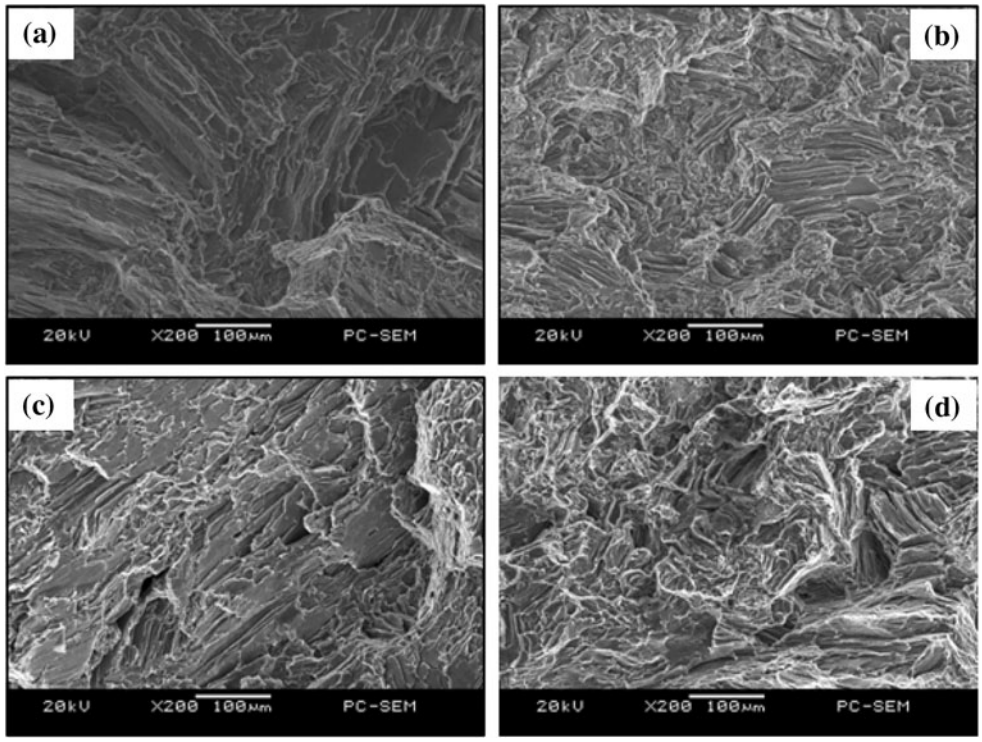

Fig. 8 SEM images of the tensile fractographs for the as-cast alloys tested at room temperature: (a) Mg-4Y-1.2Mn-1Zn; (b) Mg-4Y-1.2Mn-1Zn-0.5Zr; (c) Mg-4Y-1.2Mn-1Zn-0.1Sr; and (d) Mg-4Y-1.2Mn-1Zn-0.5Zr-0.1Sr

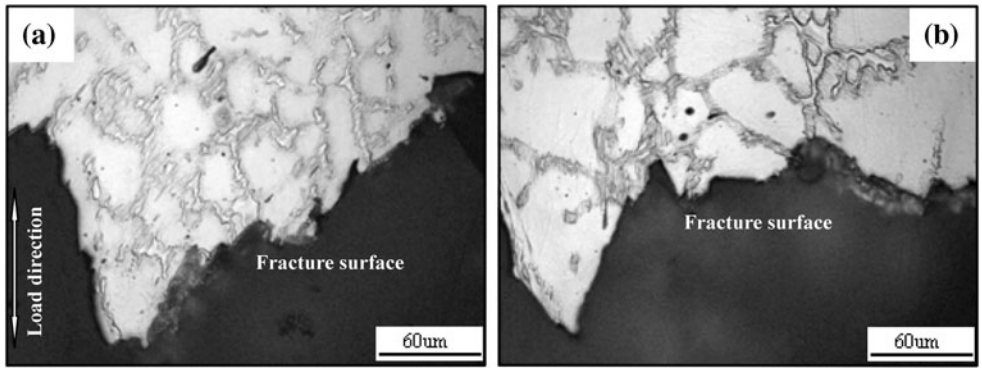

Fig. 9 Optical images of longitudinal sections for the as-cast alloys failed in tensile test at room temperature: (a) Mg-4Y-1.2Mn-1Zn; (b) Mg-4Y-1.2Mn-1Zn-0.5Zr-0.1Sr

additions of Zr and/or Sr on the tensile properties of the Mg-4Y-1.2Mn-1Zn alloy can be further confirmed from Fig. 8 and 9. Figures 8 and 9 show the SEM images, respectively, of tensile fractographs and optical images of longitudinal sections for the as-cast alloys failed in the tensile tests at room temperature. As shown in Fig. 8, a number of cleavage planes and steps are present, and some river patterns can also be observed in the tensile fracture surfaces of the experimental alloys, indicating that all the tensile fracture surfaces have mixed characteristics of cleavage and quasi-cleavage fractures. Furthermore, it is observed from Fig. 9 that the tensile rupture of the experimental alloys occurs along inter-granular boundary. Obviously, small additions of Zr and/or Sr to the Mg-4Y-1.2Mn-1Zn alloy do not significantly change the fracture mode of the alloy. However, some very obvious lacerated ridges are observed in the tensile fracture surface of the quaternary alloy. This is consistent with the relatively poor tensile properties of the quaternary alloy.

In addition, it is observed from Table 2 that the creep properties of the Zr- and/or Sr-containing alloys are similar to those of the quaternary alloy, indicating that small additions of Zr and/or Sr to the Mg-4Y-1.2Mn-1Zn alloy do not have obvious effects on the creep properties of the alloy. It is well known that the creep resistance properties of magnesium alloys are mainly related to the structural stability at high temperatures. Figure 10 shows the SEM image of the solutionized experimental alloys. It is observed from Fig. 10 that a majority of the $Mg_{12}YZn$ phases in the alloys have dissolved into the matrix after the solid solution heat treatment at 520 °C for 12 h. However, it is found that the amount of the remanent $Mg_{12}YZn$

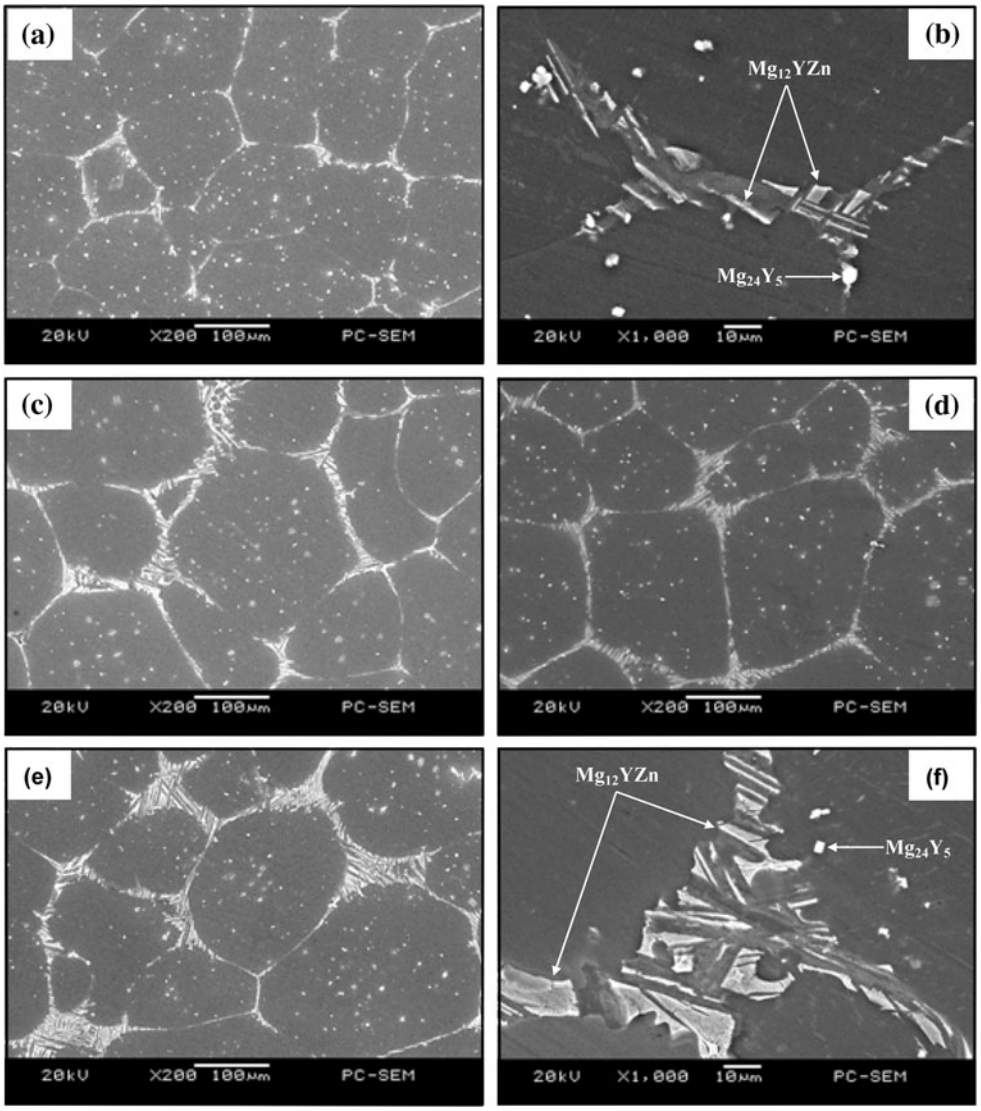

Fig. 10 SEM images of the solutionized alloys: (a, b) Mg-4Y-1.2Mn-1Zn; (c) Mg-4Y-1.2Mn-1Zn-0.5Zr; (d) Mg-4Y-1.2Mn-1Zn-0.1Sr; (e, f) Mg-4Y-1.2Mn-1Zn-0.5Zr-0.1Sr

phases at the grain boundaries for the Zr- and/or Sr-containing alloys seems to be relatively larger than that for the quaternary alloy, indicating that the thermal stability of the eutectic $Mg_{12}YZn$ phases in the Zr- and/or Sr-containing alloys is relatively higher than that in the quaternary alloy. Obviously, the effects of small additions of Zr and/or Sr on the thermal stability of the eutectic $Mg_{12}YZn$ phase cannot explain the difference in the creep properties of the experimental alloys. The difference in the creep properties is possibly related to some other mechanism. It is well known that the dispersion strengthening is one major strengthening mechanism for creep resistance of alloys (Ref 22). The second-phase particles can contribute to the creep resistance by obstructing dislocation annihilation in dislocation creep or inhibiting grain boundary migration and/or grain boundary sliding in diffusional creep. As shown in Fig. 7, the difference in the morphology, size, and distribution of the second-phase particles between the alloys, with and without the additions of Zr and/or Sr, is small. Obviously, the dispersion strengthening easily explains the similarity in the creep properties of the experimental alloys. In addition, it is generally accepted that the rate of dislocation creep tends to decrease with increasing grain size due to a decreased contribution of grain boundary sliding (Ref 22). Since the effects of small additions of Zr and/or Sr on the grain size of the Mg-4Y-1.2Mn-1Zn alloy are not completely clear, further investigations about the effect of the grain size on the creep properties need to be considered.

4. Conclusions

(1) The as-cast Mg-4Y-1.2Mn-1Zn alloys with and without the additions of Zr and/or Sr are mainly composed of α-Mg and $Mg_{12}YZn$ phases with continuous and/or quasi-continuous nets. Small additions of Zr and/or Sr to the Mg-4Y-1.2Mn-1Zn alloy do not cause an obvious change in the morphology and distribution of the $Mg_{12}YZn$ phase in the alloy.

(2) Small additions of Zr and/or Sr to the Mg-4Y-1.2Mn-1Zn alloy can improve the tensile properties at room temperature and 300 °C. Among the Zr- and/or

Sr-containing alloys, the alloy with the addition of 0.5 wt.% Zr + 0.1 wt.% Sr obtains the optimum tensile properties, followed by the alloys with the additions of 0.5 wt.% Zr and 0.1 wt.% Sr, in the respective order. However, small additions of Zr and/or Sr to the Mg-4Y-1.2Mn-1Zn alloy do not have obvious effects on the creep properties of the alloy.

Acknowledgments

This study was supported by the National Natural Science Funds of China (No. 50725413), the Major State Basic Research Development Program of China (973) (No. 2007CB613704), the Chongqing Science and Technology Commission in China (CSTC, 2010AC4085, 2009AB4134, and 2006AA4012-9-6), and the Program for Hundreds of Distinguished Leading Scientists of CQ CSTC (2010CSTC-HDLS).

References

1. M. Pekguleryuz and M. Celikin, Creep Resistance in Magnesium Alloys, *Inter. Mater. Rev.*, 2010, **55**, p 197–217
2. B.L. Mordike, I. Stulikova, and B. Smola, Mechanisms of Creep Deformation in Mg-Sc-Based Alloys, *Metal. Mater. Trans. A*, 2005, **36**, p 1729–1736
3. F.V. Buch, J. Lietzau, B.L. Mordike, A. Pisch, and R. Schmid-Fetzer, Development of Mg-Sc-Mn Alloys, *Mater. Sci. Eng. A*, 1999, **263**, p 1–7
4. B.L. Mordike, Development of Highly Creep Resistant Magnesium Alloys, *J. Mater. Proc. Technol.*, 2001, **117**, p 391–394
5. I. Stulíkova, B. Smola, F.V. Buch, and B.L. Mordike, Mechanical Properties and Creep of Mg-Rare Earth-Sc-Mn Squeeze Cast Alloys, *Materialwissenschaft und Werkstofftechnik*, 2003, **34**, p 102–108
6. B. Smola, I. Stulikova, J. Pelcova, and B.I. Mordike, Significance of Stable and Metastable Phases in High Temperature Creep Resistant Magnesium-Rare Earth Base Alloys, *J. Alloys Compd.*, 2004, **378**, p 196–201
7. B. Chen, D.L. Lin, X.Q. Zeng, and C. Lu, Effects of Yttrium and Zinc Addition on Microstructure and Mechanical Properties of Mg-Y-Zn Alloys, *J. Mater. Sci.*, 2010, **45**, p 2510–2517
8. Y.M. Zhu, A.J. Morton, and J.F. Nie, Improvement in The Age-Hardening Response of Mg-Y-Zn Alloys by Ag Additions, *Scripta Mater.*, 2008, **58**, p 525–528
9. J.Y. Lee, D.H. Kim, H.K. Lim, and D.H. Kim, Effects of Zn/Y Ratio on Microstructure and Mechanical Properties of Mg-Zn-Y Alloys, *Mater. Lett.*, 2005, **59**, p 3801–3805
10. B. Smola, I. Stulikova, J. Pelcova, and N. Zaludova, Phase Composition and Creep Behavior of Mg-RE-Mn Alloys with Zn Addition[A], *Proceedings of 7th International Conference on Magnesium Alloys and Their Applications[C]*, K.U. Kainer, Ed., Dresden, Germany, 2007, p 67–72
11. M. Yang, F. Pan, J. Shen, Y. Zhu, and C. Qin, Comparison About As-Cast Microstructures and Mechanical Properties of Mg-4Y-1.2Mn-0.9Sc and Mg-4Y-1.2Mn-1Zn (wt.%) Magnesium Alloys, *J. Mater. Sci.*, 2011. doi:10.1007/s10853-010-5188-7
12. G. Ben-Hamu, D. Eliezer, K.S. Shin, and S. Cohen, The Relation Between Microstructure and Corrosion Behavior of Mg-Y-RE-Zr Alloys, *J. Alloys Compd.*, 2007, **431**, p 269–276
13. M. Yang, F. Pan, R. Cheng, and A. Tang, Effect of Mg-10Sr Master Alloy on Grain Refinement of AZ31 Magnesium Alloy, *Mater. Sci. Eng. A*, 2008, **491**, p 440–445
14. M.S. Dargusch, S.M. Zhu, J.F. Nie, and G.L. Dunlop, Microstructural Analysis of the Improved Creep Resistance of a Die-Cast Magnesium-Aluminium-Rare Earth Alloy by Strontium Additions, *Scripta Mater.*, 2009, **60**, p 116–119
15. H.F. Zhao, L. Wang, L. Sun, S.A. Zhang, K. Yan, Q.F. Li, and M.Y. Liu, Research on the Mechanical Properties of Magnesium-Manganese-Strontium Alloy, *Mater. Res. Appl.*, 2009, **3**, p 262–264, in Chinese
16. E.F. Emley, *Principles of Magnesium Technology*, Pergamon, Oxford, 1966, p 127–155
17. M. Bamberger and G. Dehm, Trends in the Development of New Mg Alloys, *Annu. Rev. Mater. Res.*, 2008, **38**, p 505–533
18. J. Grobner and R. Schmid-Fetzer, Selection of Promising Quaternary Candidates from Mg-Mn-(Sc, Gd, Y, Zr) for Development of Creep-Resistant Magnesium Alloys, *J. Alloys Compd.*, 2001, **320**, p 296–301
19. B.L. Mordike, Creep-Resistant Magnesium Alloys, *Mater. Sci. Eng. A*, 2002, **324**, p 103–112
20. M. Yang, F. Pan, and L. Cheng, Effects of Minor Sr on As-Cast Microstructure and Mechanical Properties of ZA84 Magnesium Alloy, *J. Mater. Eng. Perform.*, 2010, **19**, p 1043–1050
21. Z.H. Huang, S.M. Liang, R.S. Chen, and E.H. Han, Solidification Pathways and Constituent Phases of Mg-Zn-Y-Zr Alloys, *J. Alloys Compd.*, 2009, **468**, p 170–178
22. S.M. Zhu, B.L. Mordike, and J.F. Nie, Creep Properties of a Mg-Al-Ca Alloy Produced by Different Casting Technologies, *Mater. Sci. Eng. A*, 2008, **483–484**, p 583–586